Alkyne Adducts of Ditungsten Tetrapivalate: $[W_2(\kappa^2\text{-}O_2C^tBu)_4(\mu\text{-}RCCR')_2]$, Where R = R′ = Me, Et, Ph and R = Me, R′ = Ph

Matthew J. Byrnes, Malcolm H. Chisholm,* Judith Gallucci, and Paul J. Wilson†

Department of Chemistry, Newman & Wolfrom Laboratories, The Ohio State University, 100 West 18th Avenue, Columbus Ohio, 43210-1185

Received January 30, 2002

Aromatic hydrocarbon solutions of $[W_2(O_2C^tBu)_4]$ react with alkynes RC≡CR′ to give adducts of the formula $[W_2(\kappa^2\text{-}O_2C^tBu)_4(\mu\text{-}RCCR')_2]$, where R = R′ = Me, Et, Ph and R = Me, R′ = Ph, as orange to purple air-stable, hydrocarbon-soluble, crystalline solids which have been characterized by infrared, NMR spectroscopy, and mass spectrometry. The single-crystal X-ray structures have also been obtained for R = R′ = Me and R = Me, R′ = Ph. In both structures, there are a pair of perpendicularly bridged alkyne ligands with central C−C distances of ca. 1.34 Å and a W−W bond of ca. 2.5 Å. The crystallographically characterized molecules have virtual C_{2h} symmetry, and in solution, the NMR data are consistent with the presence of this isomer and a second having D_2 symmetry. The two isomers can be related to *meso* and Δ/Λ isomers of an edge-bridged octahedral unit containing four chelates: $[(chelate)_2M(\mu\text{-}X)_2M(chelate)_2]$, where X represents the central position of the μ-perpendicular alkyne. The isomerization in solution was found to be intramolecular and solvent-assisted, with THF-d_8 > benzene-d_6 ≈ toluene-d_8 > CD_2Cl_2, and can be catalyzed by the addition of $^tBuCO_2H$. The electronic structure and bonding in these compounds have been investigated using density functional theory calculations on the model compounds D_2 and C_{2h} $[W_2(\kappa^2\text{-}O_2\text{-}CH)_4(\mu\text{-}HCCH)_2]$. These calculational results lend credence to the notion that there is a W−W bond of order 2.

Introduction

Addition of alkynes to metal−metal triply bonded compounds has yielded an extensive field of organometallic chemistry ranging from simple alkyne adducts of carbonyl complexes such as $[Cp_2M_2(CO)_4]$[1−6] and alkoxide complexes such as $[M_2(OR)_6]$ (M = Mo, W)[7−9] to C−C-coupled products, e.g. $[W_2(O^iPr)_6(\mu\text{-}C_4Me_4)(\eta^2\text{-}MeCCMe)]$,[10] and products of scission or metathesis, e.g. $[(^tBuO)_3W{\equiv}CR]$ (R = Me, Et, ^{n}Pr, etc.).[11−14] In contrast, the chemistry involving alkynes and M−M quadruple bonds remains relatively unexplored. Indeed, to our knowledge, the only well-documented products have been derived from the reactions between terminal alkynes and $[Mo_2(O_2CMe)_4]$ in ethylenediamine, which have been shown to labilize the bridging carboxylate ligands: $[Mo_2(en)_4(\mu,\kappa^1\text{-}O_2CMe)(\mu\text{-}RCCH)][MeCO_2]_3$.[15] Recognizing the highly reactive nature of the W−W quadruple bond in $[W_2(O_2C^tBu)_4]$,[16] we undertook a study of its reactions with alkynes and describe herein our findings.

Results and Discussion

Syntheses. Addition of ethyne or propyne to aromatic (benzene or toluene) solutions of $[W_2(O_2C^tBu)_4]$ at room temperature followed by heating to 70 °C yielded dark intractable solids, presumably polyacetylenes, and unreacted $[W_2(O_2C^tBu)_4]$. Addition of MeC≡CMe or EtC≡CEt under similar conditions also yielded dark products, from which the orange crystalline compounds $[W_2(\kappa^2\text{-}O_2C^tBu)_4(\mu\text{-}RCCR)_2]$ (R = Me, Et) were extracted with hexanes. A similar reaction occurred with PhC≡CR, yielding red (R = Me) and purple (R = Ph) compounds. No reaction was observed for $Me_3SiC{\equiv}CSiMe_3$, presum-

* To whom correspondence should be addressed. E-mail: chisholm@chemistry.ohio-state.edu.
† Current address: Department of Chemistry, University of Bath, Bath BA2 7AY, U.K.

(1) Klingler, R. J.; Butler, W.; Curtis, M. D. *J. Am. Chem. Soc.* **1975**, *97*, 3535−3536.
(2) Bailey, W. I., Jr.; Chisholm, M. H.; Cotton, F. A.; Rankel, L. A. *J. Am. Chem. Soc.* **1978**, *100*, 5764−5773.
(3) Ginley, D. S.; Bock, C. R.; Wrighton, M. S. *Inorg. Chim. Acta* **1977**, *23*, 85−94.
(4) Knox, S. A. R.; Stansfield, R. F. D.; Stone, F. G. A.; Winter, M. J.; Woodward, P. *J. Chem. Soc., Chem. Commun.* **1978**, 221−223.
(5) Beck, J. A.; Knox, S. A. R.; Stansfield, R. F. D.; Stone, F. G. A.; Winter, M. J.; Woodward, P. *J. Chem. Soc., Dalton Trans.* **1982**, 195−200.
(6) Gerlach, R. F.; Duffy, D. N.; Curtis, M. D. *Organometallics* **1983**, *2*, 1172−1178.
(7) Chisholm, M. H.; Folting, K.; Huffman, J. C.; Rothwell, I. P. *J. Am. Chem. Soc.* **1982**, *104*, 4389−4399.
(8) Chisholm, M. H.; Folting, K.; Hoffman, D. M.; Huffman, J. C. *J. Am. Chem. Soc.* **1984**, *106*, 6794−6805.
(9) Chisholm, M. H.; Conroy, B. K.; Clark, D. L.; Huffman, J. C. *Polyhedron* **1988**, *7*, 903−918.
(10) Chisholm, M. H.; Hoffman, D. M.; Huffman, J. C. *J. Am. Chem. Soc.* **1984**, *106*, 6806−6815.
(11) Schrock, R. R.; Listemann, M. L.; Sturgeoff, L. G. *J. Am. Chem. Soc.* **1982**, *104*, 4291−4293.
(12) Listemann, M. L.; Schrock, R. R. *Organometallics* **1985**, *4*, 74−83.
(13) Wengrovius, J. H.; Sancho, J.; Schrock, R. R. *J. Am. Chem. Soc.* **1981**, *103*, 3932−3934.
(14) Sancho, J.; Schrock, R. R. *J. Mol. Catal.* **1982**, *15*, 75−79.
(15) Kerby, M. C.; Eichhorn, B. W.; Doviken, L.; Vollhardt, K. P. C. *Inorg. Chem.* **1991**, *30*, 156−158.
(16) Santure, D. J.; Huffman, J. C.; Sattelberger, A. P. *Inorg. Chem.* **1985**, *24*, 371−378.

10.1021/om020074e CCC: $22.00
Publication on Web 04/23/2002

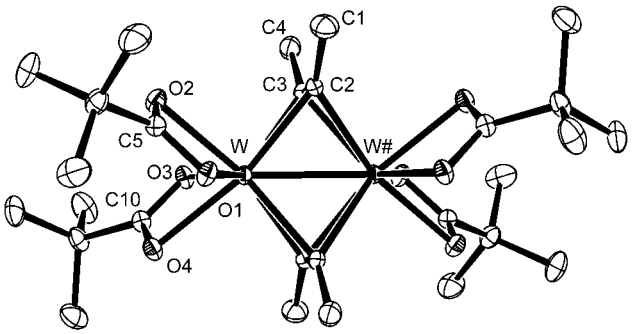

Figure 1. ORTEP drawing of $[W_2(\kappa^2\text{-}O_2C^tBu)_4(\mu\text{-}MeC\text{-}CMe)_2]$ giving the atom-numbering scheme used in the tables. The atoms are drawn with 50% probability displacement ellipsoids. All hydrogen atoms have been omitted for clarity.

Table 1. Selected Bond Distances (Å) and Bond Angles (deg) for $[W_2(\kappa^2\text{-}O_2C^tBu)_4(\mu\text{-}MeCCMe)_2]$

A−B	dist	A−B	dist
W−W#[a]	2.4888(2)	W#−C(2)	2.154(2)
W−O(1)	2.119(2)	W−C(3)	2.140(2)
W−O(2)	2.223(2)	W#-C(3)	2.142(2)
W−O(3)	2.123(2)	W−C(5)	2.549(2)
W−O(4)	2.225(2)	W−C(10)	2.549(2)
W−C(2)	2.154(2)	C(3)−C(4)	1.489(3)
A−B−C	**angle**	**A−B−C**	**angle**
O(1)−W−O(2)	59.82(6)	C(1)−C(2)−C(3)	137.0(2)
O(3)−W−O(4)	59.84(6)	C(2)−C(3)−C(4)	139.5(2)
C(5)−W−C(10)	89.79(7)	C(2)−W−C(3)	36.37(9)
C(2)−W−C(5)	87.99(8)		

[a] # denotes atoms generated by the symmetry operation $-x + 1, -y, -z$.

ably due to steric factors. Addition of 1 equiv of alkyne only yielded the 2:1 alkyne adduct and unreacted $[W_2(O_2C^tBu)_4]$. No further reactions were observed for the $[W(\kappa^2\text{-}O_2C^tBu)_4(\mu\text{-}RCCR)_2]$ compounds in the presence of excess RC≡CR. There was also no observed reaction between $[W_2(\kappa^2\text{-}O_2C^tBu)_4(\mu\text{-}MeCCMe)_2]$ with PhC≡CPh in toluene.

The isolated $[W_2(\kappa^2\text{-}O_2C^tBu)_4(\mu\text{-}RCCR')_2]$ compounds are notably more stable to the atmosphere (O_2, H_2O) than $[W_2(O_2C^tBu)_4]$. Indeed, the compounds can be handled in the air both in the solid state and in solution for short periods of time. The IR spectra (KBr) for each of the isolated solids $[W_2(\kappa^2\text{-}O_2C^tBu)_4(\mu\text{-}RCCR')_2]$ (R = R′ = Me, Ph; R = Me, R′ = Ph), show two strong absorptions at ca. 1510 and 1431 cm^{-1}. These bands are probably due to the $\nu_a(CO_2)$ and $\nu_s(CO_2)$ bands of the pivalate groups.[17] The expected $\nu(C{\equiv}C)$ band for the bis-PhC≡CMe adduct could not be detected.

Single-Crystal and Molecular Structures. $[W_2(\kappa^2\text{-}O_2C^tBu)_4(\mu\text{-}MeCCMe)_2]$. An ORTEP drawing of the molecule is given in Figure 1, and selected bond distances and angles are given in Table 1. The molecule has a crystallographically imposed center of inversion. The W−W distance of 2.4888(2) Å is in the range seen for W═W distances,[18] and the coordinated alkyne central C−C distance of 1.344(3) Å is comparable to that in ethylene (1.339(1) Å),[19] although notably shorter than

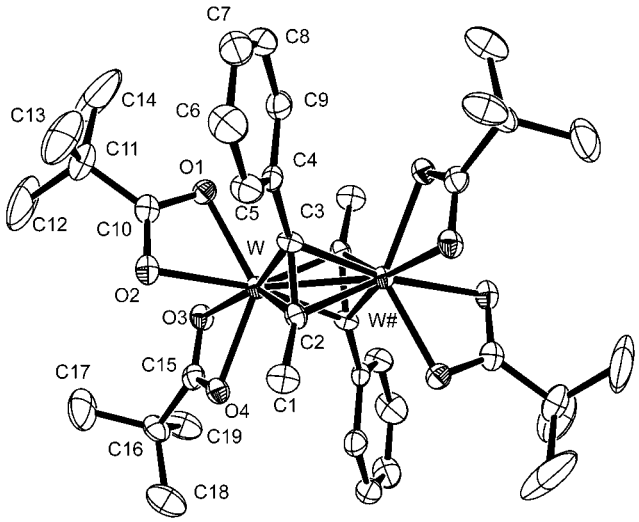

Figure 2. ORTEP drawing of $[W_2(\kappa^2\text{-}O_2C^tBu)_4(\mu\text{-}PhC\text{-}CMe)_2]$ giving the atom-numbering scheme used in the tables. The atoms are drawn with 50% probability displacement ellipsoids. All hydrogen atoms have been omitted for clarity.

Table 2. Selected Bond Distances (Å) and Bond Angles (deg) for $[W_2(\kappa^2\text{-}O_2C^tBu)_4(\mu\text{-}PhCCMe)_2]$

A−B	dist	A−B	dist
W−W#[a]	2.4925(2)	W#−C(2)	2.137(3)
W−O(1)	2.120(2)	W−C(3)	2.143(3)
W−O(2)	2.208(3)	W#-C(3)	2.171(3)
W−O(3)	2.209(2)	W−C(10)	2.550(3)
W−O(4)	2.1181(9)	W−C(15)	2.546(3)
W−C(2)	2.126(3)	C(3)−C(4)	1.348(4)
A−B−C	**angle**	**A−B−C**	**angle**
O(1)−W−O(2)	60.02(8)	C(1)−C(2)−C(3)	138.1(3)
O(3)−W−O(4)	59.90(8)	C(2)−C(3)−C(4)	138.4(2)
C(10)−W−C(15)	93.62(10)	C(2)−W−C(3)	36.81(11)

[a] # denotes atoms generated by the symmetry operation $-x, -y, -z$.

in alkyne adducts of $[W_2(OR)_6]$.[8−10] The C−C−C angle of the bridging alkyne is ca. 137°, which is close to that of an sp^2-hybridized carbon, clearly implying extensive bonding to the ditungsten center. The W−O distances of the chelating pivalate ligands span a narrow range of 2.12−2.25 Å.

$[W_2(\kappa^2\text{-}O_2C^tBu)_4(\mu\text{-}PhCCMe)_2]$. An ORTEP drawing of this centrosymmetric molecule is given in Figure 2, and selected bond distances and angles are given in Table 2. The structural parameters of this molecule closely parallel those of the dimethylacetylene complex described above, and thus, the pair of structurally characterized molecules most surely will be representative of the class of compounds of formula $[W_2(\kappa^2\text{-}O_2C^tBu)_4(\mu\text{-}RCCR')_2]$.

The drawings of the molecules given in Figures 1 and 2 indicate that each tungsten can be viewed as eight-coordinate, having four W−O and four W−C bonds. However, this interpretation of the structure was not helpful to an interpretation of the dynamic NMR behavior observed in solution (vide infra). A simplified view of the structure can be based upon the consider-

(17) Nakamoto, K. *Infrared and Raman Spectra of Inorganic and Coordination Compounds, Part B: Applications in Coordination, Organometallic, and Bioinorganic Chemistry*, 5th ed.; Wiley: New York, 1997.

(18) Cotton, F. A.; Walton, R. A. *Multiple Bonds Between Metal Atoms*, 2nd ed.; Oxford University Press: Oxford, U.K., 1993.

(19) Duncan, J. L.; Wright, I. J.; Van Lerberghe, D. *J. Mol. Spectrosc.* **1972**, *42*, 463−477.

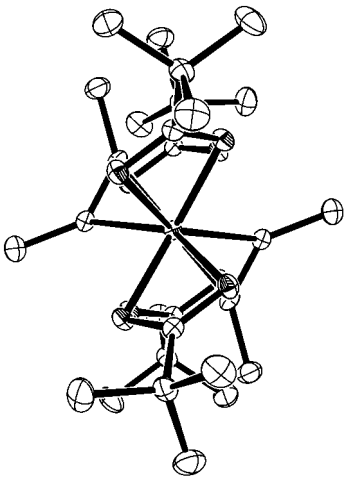

Figure 3. ORTEP drawing of $[W_2(\kappa^2\text{-}O_2C^tBu)_4(\mu\text{-}MeCCMe)_2]$ down the W−W axis, showing the different alkyne carbons and their attendant methyl groups. All hydrogen atoms have been omitted for clarity.

ation of the μ-alkyne occupying a single site such that the dinuclear molecule can be represented as an edge-shared biooctahedron, as shown in the schematic drawing **A**.

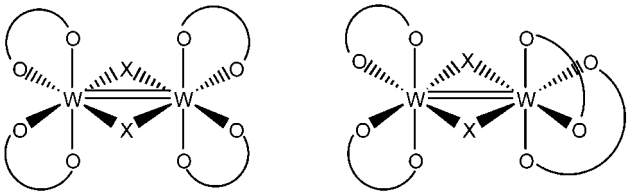

A **B**

The representation of the solid-state molecular structure by **A** emphasizes that, with a center of inversion, one has a *meso* molecule: if one tungsten is Δ, the other is Λ. As we show below, in solution, the *meso* isomers can exist in equilibrium with the pair of optically active related enantiomers having Δ,Δ and Λ,Λ symmetry of the type shown for one enantiomer by **B**.

NMR Solution Behavior. The ^{1}H NMR spectra of $[W_2(\kappa^2\text{-}O_2C^tBu)_4(\mu\text{-}MeCCMe)_2]$ recorded in toluene-d_8, benzene-d_6, CD_2Cl_2, and THF-d_8 at ambient temperature varied with time came to an equilibrium which showed three singlets for the methyl groups of the bridging MeC≡CMe ligand and two singlets for the ^{t}Bu protons. The position of equilibrium can be traced to the isomerization of **A** with **B** (and its mirror image **B′**) and is somewhat solvent-dependent. The ratio of **A** to **B** isomers of the MeC≡CMe adduct in benzene-d_6 and CD_2Cl_2 after several days at room temperature was 0.75:0.25 and 0.58:0.42, respectively. Also, the rate of isomerization is solvent-dependent with THF ≫ toluene ≈ benzene > CH_2Cl_2. The addition of a trace of free pivalic acid in CD_2Cl_2 was found to promote facile isomerization: an equilibrium mixture was established within minutes rather than days.

What is not so obvious from the molecular drawings shown in Figure 1 is that the μ-MeCCMe ligand has inequivalent Me groups. However, if the molecule is viewed down the W−W axis, as is shown in Figure 3, this inequivalence becomes clear. For the enantiomers represented by **B** and **B′**, there is only one methyl group

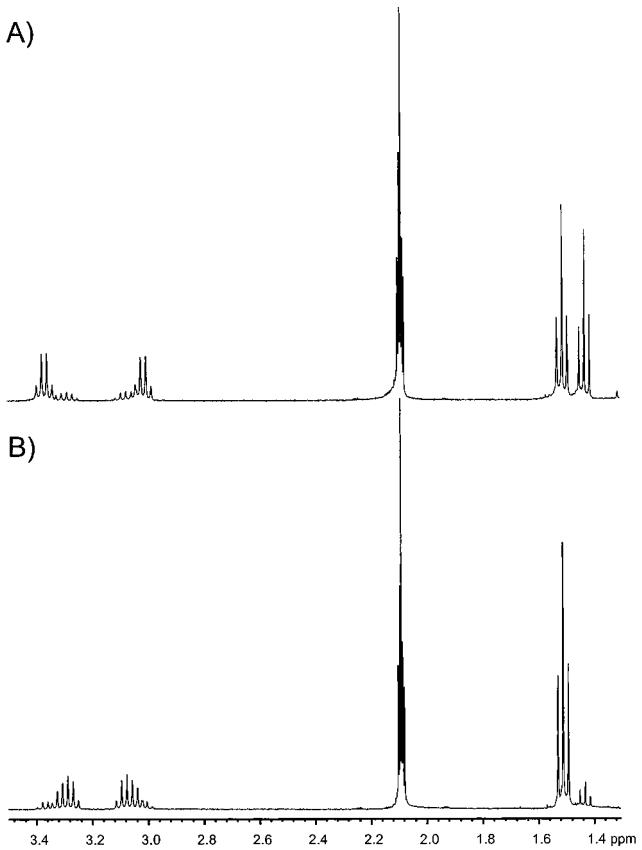

Figure 4. ^{1}H NMR spectra showing the ethyl proton resonances of $[W_2(\kappa^2\text{-}O_2C^tBu)_4(\mu\text{-}EtCCEt)_2]$ recorded at room temperature in toluene-d_8 at 400 MHz: (A) immediately after dissolving the solid; (B) after 12 h. The quintet at δ 2.09 ppm is due to the residual protio impurities of toluene-d_8.

environment. Also in the $^{13}C\{^1H\}$ NMR spectra, we observed two ^{13}C signals for the μ-C_2 carbons associated with the *meso* isomer **A**, each having slightly different $^{183}W-^{13}C$ coupling constants, whereas for the enantiomers represented by **B** and **B′**, there is a single ^{13}C resonance flanked by two sets of ^{183}W satellites.

The ^{1}H NMR spectra obtained for $[W_2(\kappa^2\text{-}O_2C^tBu)_4(\mu\text{-}EtCCEt)_2]$ are complementary to those described above. Initially, the predominant isomer has two CH_3 triplets and two CH_2 quartets, but with time, the spectra change to favor one ethyl group, which appears as an ABX_3 spin system, as shown in Figure 4.

The compound with the bridging PhC≡CMe ligand has potentially an additional set of isomers resulting from the relative positions of the Ph and Me groups, as depicted schematically by **C** and **D**. In **D**, there would

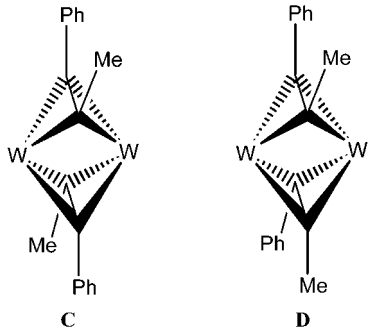

C **D**

be two types of pivalate ligands, whereas for **C**, with a center of inversion, there would be just one. This is true for both the *meso* isomer represented by **A** and the enantiomeric pair (**B** and **B′**).

The ^{1}H NMR spectrum recorded for $[W_2(\kappa^2\text{-}O_2C^tBu)_4(\mu\text{-}PhCCMe)_2]$ initially shows a single methyl signal for the bridging alkyne and a single signal for the pivalate protons. This spectrum is consistent with expectations based on the molecular structure shown in Figure 2. With time, a new Me signal grows in for the μ-PhCCMe ligand, along with *two* pivalate signals of equal intensity. This, we propose, is consistent with an isomerization of the type previously described and is not consistent with isomerization involving the bridging alkyne groups, as depicted by a conversion of **C** to **D**.

The ^{1}H NMR spectra for the isolated bis(diphenylacetylene) adduct $[W_2(\kappa^2\text{-}O_2C^tBu)_4(\mu\text{-}PhCCPh)_2]$ seems to consist mainly of the racemic (**B** or **B′**) isomers; there is no detectable isomerization from **A** to **B** or vice versa in either CD_2Cl_2 or benzene-d_6. The *meso* isomer (**A**) is detected when the reaction between $[W_2(O_2C^tBu)_4]$ and excess PhC≡CPh is followed by ^{1}H NMR spectroscopy in C_6D_6. Thus, it appears that the *meso* isomer is favored in the solid state, which is in contrast to the other bis(alkyne) adducts isolated and probably reflects the small energy differences between the *meso* and *rac* isomers of $[W_2(\kappa^2\text{-}O_2C^tBu)_4(\mu\text{-}RCCR')_2]$ (R = R′, R ≠ R′) (see below).

Bonding Considerations. It is always satisfying when one can look at a molecule and, on the basis of simple considerations of symmetry and electron counting, visualize the salient features of the bonding. For dimeric metal complexes the fragment molecular orbital approach is often useful. The relatively low symmetry and the difficulty in anticipating the relative importance of various metal−ligand interactions prevent such a simple approach here. We therefore undertook molecular orbital calculations for the model species $[W_2(\kappa^2\text{-}O_2CH)_4(\mu\text{-}MeCCMe)_2]$ with the aid of density functional theory and the Gaussian 98 package.[20] As a starting point, we took the coordinates from the central $[W_2(\kappa^2\text{-}O_2C)_4(\mu\text{-}MeCCMe)_2]$ skeleton found for the tetrapivalate complex idealized to C_{2h} symmetry. Subsequent geometry optimizations under C_{2h} symmetry gave the calculated metrical parameters given in Table 3. A comparison of the observed and calculated distances and angles for the experimentally observed $[W_2(\kappa^2\text{-}O_2C^tBu)_4(\mu\text{-}MeCCMe)_2]$ and the formate model show reasonable agreement. A molecular orbital energy level diagram for the frontier molecular orbitals for the tetraformate model is given in Figure 5, and orbital plots for the frontier MOs are given in Figures 6 and 7.

The HOMO is clearly W_2 to $(C_2)_2$ π-bonding—one of the combinations encompassing the W_2 dπ to alkyne π* back-bonding anticipated in the earlier description. HOMO−1 is also clearly M−M σ-bonding with some M−C σ-bonding character. The next three molecular orbitals all lie more than l eV lower in energy. HOMO−2 is an orbital that has essentially no formate character but can be viewed as a mixture of M−M δ and M_2 to C_2 π*-back-bonding. HOMO−3 and HOMO can be considered as in- and out-of-phase combinations of M−M δ and C_2 π*-combinations. Both are M−C bonding and contribute toward a four-electron reduction of the two alkynes, which is equivalent to a two-electron reduction of each. HOMO−3 is M−M π-bonding with some admixture of both alkyne and formate orbitals. HOMO−4 is alkyne C_2 pπ to W_2 σ-bonding. The low symmetry of the molecule clearly means the C_2 to W_2 interaction involves only one of the alkyne carbon atoms of each C_2 moiety. HOMO−5 is a filled C_2 π to W_2 σ-interaction.

The highest six occupied molecular orbitals comprise the principal interactions between the W_2 and bridging

Table 3. Calculated Distances (Å) and Angles (deg) for the C_{2h} Isomer of $[W_2(\kappa^2\text{-}O_2CH)_4(\mu\text{-}MeCCMe)_2]$

A−B	dist	A−B	dist
W−W	2.526	W−C_{alkyne}	2.176
W−O	2.166		2.184
	2.288	C_{alkyne}−C_{alkyne}	1.35

A−B−C	angle	A−B−C	angle
C_{methyl}−C_{alkyne}−C_{alkyne}	138.6	C_{alkyne}−W−C_{alkyne}	36.1
	137.5	C_a−W−C_a[a]	91.7

[a] C_a = formate carboxylate carbon.

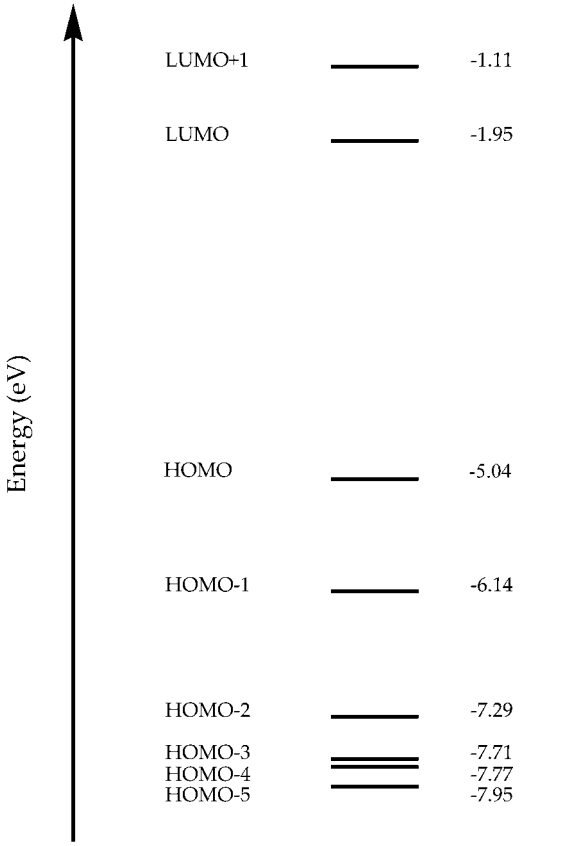

Figure 5. Schematic molecular orbital energy level diagram for the frontier molecular orbitals of C_{2h}-$[W_2(\kappa^2\text{-}O_2CH)_4(\mu\text{-}MeCCMe)_2]$.

(20) Frisch, M. J.; Trucks, G. W.; Schlegel, H. B.; Scuseria, G. E.; Robb, M. A.; Cheeseman, J. R.; Zakrzewski, V. G.; Montgomery, J. A., Jr.; Stratmann, R. E.; Burant, J. C.; Dapprich, S.; Millam, J. M.; Daniels, A. D.; Kudin, K. N.; Strain, M. C.; Farkas, O.; Tomasi, J.; Barone, V.; Cossi, M.; Cammi, R.; Mennucci, B.; Pomelli, C.; Adamo, C.; Clifford, S.; Ochterski, J.; Petersson, G. A.; Ayala, P. Y.; Cui, Q.; Morokuma, K.; Malick, D. K.; Rabuck, A. D.; Raghavachari, K.; Foresman, J. B.; Cioslowski, J.; Ortiz, J. V.; Stefanov, B. B.; Liu, G.; Liashenko, A.; Piskorz, P.; Komaromi, I.; Gomperts, R.; Martin, R. L.; Fox, D. J.; Keith, T.; Al-Laham, M. A.; Peng, C. Y.; Nanayakkara, A.; Gonzalez, C.; Challacombe, M.; Gill, P. M. W.; Johnson, B. G.; Chen, W.; Wong, M. W.; Andres, J. L.; Head-Gordon, M.; Replogle, E. S.; Pople, J. A. *Gaussian 98*; Gaussian, Inc.: Pittsburgh, PA, 1998.

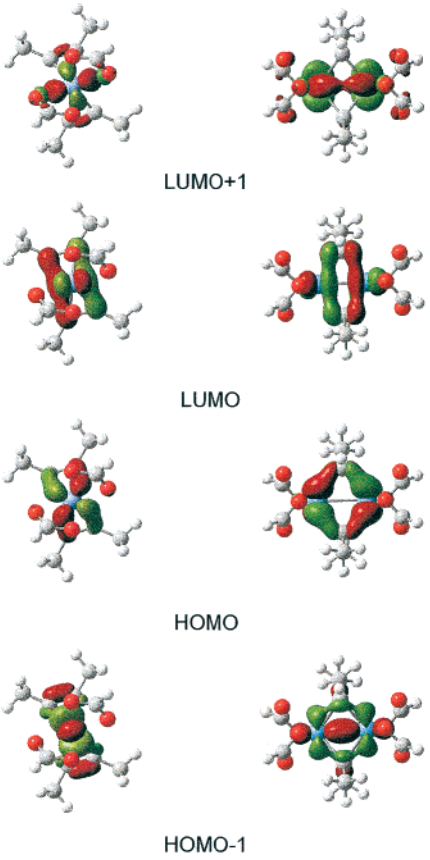

Figure 6. GaussView representations of LUMO+1, LUMO, HOMO, and HOMO−1 of $[W_2(\kappa^2\text{-}O_2CH)_4(\mu\text{-}MeCCMe)_2]$ viewed both along and perpendicular to the W−W axis.

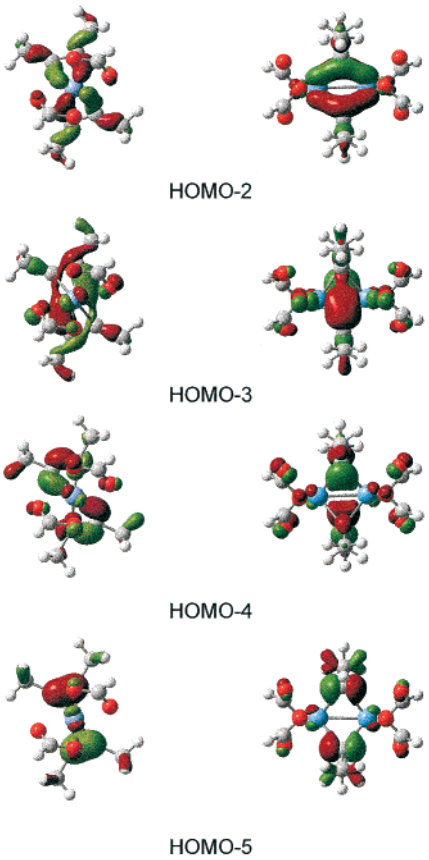

Figure 7. GaussView representations of HOMO−2, HOMO−3, HOMO−4 and HOMO−5 of $[W_2(\kappa^2\text{-}O_2CH)_4(\mu\text{-}MeCCMe)_2]$ viewed both along and perpendicular to the W−W axis.

C_2 units. It becomes clearer from these orbitals that each alkyne effectively donates an electron pair to the W_2 moiety and each alkyne receives an electron pair in back-bonding. Also from the orbital plots of the HOMO−4 orbital we can understand why the bridging alkyne carbons have two different couplings to ^{183}W ($I = {}^1/_2$). For each alkyne there are two acetylenic carbons and each is bonded differently to both tungsten atoms. This view of the bonding is consistent with the observed C−C and W−C distances and the C−C−C angles for the bridging alkyne. Of the occupied frontier molecular orbitals, those having significant M−M bonding character are HOMO−1, which is M−M σ, HOMO−2, which is in principle M−M δ, and HOMO−3 and −4, which are M−M π, but all have significant mixing with the bridging alkyne orbitals. However, with the involvement of four MOs with M−M bonding character it is not surprising that the M−M distance falls within the range commonly seen for W−W double bonds. Indeed, the distance may be compared with that seen for $[W_2Cl_4(OEt)_4(HOEt)_2]$, which adopts a more bona fide edge-shared bioctahedral geometry (2.43(1) Å).[21,22]

The LUMO is an admixture of M−M d_π−d_π and C−C p_π antibonding orbitals, and LUMO+1, which is not much higher in energy, is M−M δ in character with relatively small contribution from either the alkyne or formate. The calculated HOMO−LUMO gap is nearly 3 eV, which is consistent with the orange color that arises from absorption in the UV region of the spectrum which tails into the visible.

We have also calculated the optimized geometries for model ethyne-bridged complexes $[W_2(\kappa^2\text{-}O_2CH)_4(\mu\text{-}HCCH)_2]$ under both C_{2h} and D_2 symmetry. The D_2 species models the racemic isomers that we propose exist in solution in equilibrium with the C_{2h} isomer. The frontier orbitals of the ethyne adduct were essentially identical with those described for the C_{2h} dimethylacetylene complex, while the energy difference between the C_{2h} and D_2 isomers was less than 1 kcal mol^{-1} with the D_2 isomer being lower in energy. A view of the calculated energy minimized geometry for the D_2 isomer along with selected metric parameters is given in Figure 8.

Concluding Remarks

The present work opens a new chapter in the organometallic chemistry associated with W−W quadruple bonds. It is interesting that the reactions reported here yield bis(alkyne) adducts, in contrast to alkyne addition to M−M triply bonded compounds of tungsten, which yield mono(alkyne) adducts or products of C−C scission or C−C coupling. However, as we noted in the Introduction, a single alkyne adduct to a Mo−Mo quadruple bond was reported by Eichhorn and co-workers[15] and presumably in the reactions reported here a species having

(21) Anderson, L. B.; Cotton, F. A.; DeMarco, D.; Fang, A.; Ilsley, W. H.; Kolthammer, B. W. S.; Walton, R. A. *J. Am. Chem. Soc.* **1981**, *103*, 5078−5086.
(22) Cotton, F. A.; Falvello, L. R.; Fredrich, M. F.; DeMarco, D.; Walton, R. A. *J. Am. Chem. Soc.* **1983**, *105*, 3088−3097.

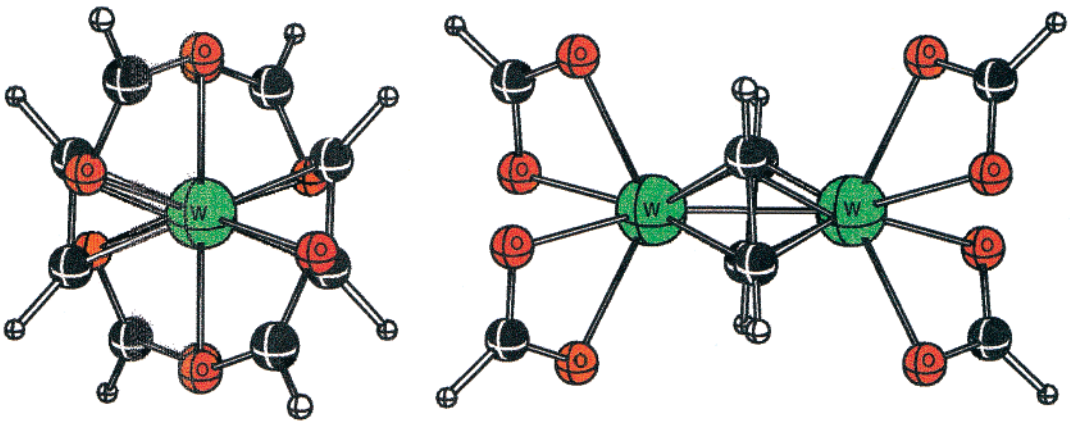

Figure 8. Two views of the calculated D_2-[$W_2(\kappa^2$-$O_2CH)_4(\mu$-HCCH)$_2$] isomer. The calculated distances and angles are as follows: W−W = 2.537 Å, W−O = 2.163 and 2.268 Å, W−C = 2.146 and 2.201 Å, C−C = 1.346 Å, ∠C−C−H = 138.2°.

a similar structure, namely that shown in **E**, could be a

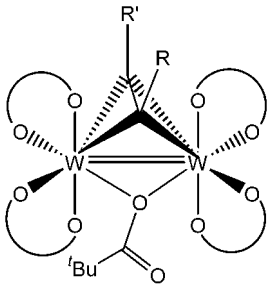

E

reaction intermediate. The only other compounds that would seem related to the ones described here are [$W_2(OR)_4(\mu$-R′CCR′$)_2$] (R = ^{i}Pr, ^{t}Bu) but these were obtained by addition-elimination reactions involving [$W_2{}^n$Pr$_2$(O^iPr)$_4$] and [$W_2(O^t$Bu)$_6$].[23]

Experimental Section

Physical Measurements. NMR spectra were recorded on a 400 MHz Bruker DPX Avance^{400} spectrometer. All ^{1}H NMR chemical shifts are reported in ppm relative to the ^{1}H impurity as follows: methylene chloride-d_2, triplet at 5.32 ppm; benzene-d_6, singlet at 7.15 ppm; toluene-d_8, quintet at 2.09 ppm; thf-d_8, broad multiplet at 3.58 ppm. ^{13}C NMR chemical shifts are reported in ppm relative to the CD_2Cl_2 triplet of methylene chloride-d_2 at δ 53.8, to the C_6D_6 triplet of benzene-d_6 at δ 128.0, or to the methyl septet of toluene-d_8 at δ 20.4. Electron impact (EI) mass spectra were collected on a Kratos MS890 double-focusing magnetic mass spectrometer, and electrospray ionization (ESI) mass spectra were collected on an Esquire-LC 00049 spectrometer. Microanalyses were carried out by Atlantic Microlab, Inc.

Synthesis. All reactions were carried out under an atmosphere of oxygen-free UHP-grade argon using standard Schlenk techniques or under a dry and oxygen-free nitrogen atmosphere using standard glovebox techniques. All solvents were dried and degassed by standard methods and distilled prior to use. Ditungsten tetrapivalate was prepared by the literature procedure.[16] 2-Butyne, 3-hexyne, 1-phenyl-1-propyne, and diphenylacetylene were purchased from commercial sources and used as received.

As all four bis(alkyne) adducts were synthesized using the same methodology, only the preparation of [$W_2(\kappa^2$-O_2C^tBu)$_4$-(μ-MeCCMe)$_2$] is described in detail.

Preparation of [$W_2(\kappa^2$-O_2C^tBu)$_4(\mu$-MeCCMe)$_2$]. [$W_2(O_2C^t$-Bu)$_4$] (520 mg, 0.67 mmol) was dissolved in benzene (ca. 100 mL) in a Schlenk flask in the drybox. The flask was removed from the drybox and attached to a Schlenk line, and 2-butyne (ca. 200 μL, 2.56 mmol) was added via a microsyringe. The flask was heated to 70 °C for 16 h, during which time the solution changed to orange-brown. An orange solid was obtained after removal of the volatiles in vacuo and addition of hexanes (20 mL). The supernatant was carefully decanted off and the solid washed several times with small amounts of hexanes. A second crop of the orange material was isolated from the slow evaporation of the brown hexanes solution. X-ray-quality crystals were grown by the slow evaporation of a hexanes solution. The total mass of orange solid isolated was 236 mg (40% yield).

Anal. Found: C, 38.28; H, 5.38. Calcd for $C_{28}H_{48}O_8W_2$: C, 38.20; H, 5.50. IR (KBr): $\nu_a(CO_2)$ 1509 cm^{-1}, $\nu_s(CO_2)$ 1431 cm^{-1}. ^{1}H NMR (C_6D_6; 400 MHz): isomer **A**, δ 1.14 (s, 36 H, $O_2CC(CH_3)_3$), 2.60 and 2.83 (both s, 6 H each, C≡CCH_3); isomer **B**, δ 1.10 (s, 36 H, $O_2CC(CH_3)_3$), 2.72 (s, 12 H, C≡CCH_3). ^{13}C NMR (C_6D_6; 100.6 MHz): isomer **A**, δ 16.63 and 19.47 (both s, C≡CCH_3), 26.58 (s, $O_2CC(CH_3)_3$), 40.38 (s, $O_2CC(CH_3)_3$), 180.18 (s, J_{WC} = 26.5, C≡CCH$_3$), 183.53 (s, J_{WC} = 32.4, C≡CCH$_3$), 196.88 (s, $O_2CC(CH_3)_3$); isomer **B**, δ 17.98 (s, C≡CCH_3), 26.53 (s, $O_2CC(CH_3)_3$), 40.34 (s, $O_2CC(CH_3)_3$), 182.43 (s, C≡CCH$_3$, J_{WC} = 24 and 35 Hz), 196.80 (s, $O_2CC(CH_3)_3$). ^{1}H NMR (CD_2Cl_2; 400 MHz): isomer **A**, δ 1.14 (s, 36 H, $O_2CC(CH_3)_3$), 2.60 and 2.83 (both s, 6 H each, C≡CCH_3); isomer **B**, δ 1.15 (s, 36 H, $O_2CC(CH_3)_3$), 2.72 (s, 12 H, C≡CCH_3). 13C NMR (CD_2Cl_2; 100.6 MHz): isomer **A**, δ 16.63 and 19.47 (both s, C≡CCH_3), 26.58 (s, $O_2CC(CH_3)_3$), 40.38 (s, $O_2CC(CH_3)_3$), 180.18 (s, J_{WC} = 27, C≡CCH$_3$), 183.53 (s, J_{WC} = 35, C≡CCH$_3$), 196.88 (s, $O_2CC(CH_3)_3$); isomer **B**, δ 17.98 (s, C≡CCH_3), 26.53 (s, $O_2CC(CH_3)_3$), 40.34 (s, $O_2CC(CH_3)_3$), 182.43 (s, J_{WC} = 24 and 35 Hz, C≡CCH$_3$), 196.80 (s, $O_2CC(CH_3)_3$). MS (ESI): *m/z* 903 (100%) $(M + Na)^+$.

Preparation of [$W_2(\kappa^2$-O_2C^tBu)$_4(\mu$-EtCCEt)$_2$]. A 422 mg portion of [$W_2(O_2C^t$Bu)$_4$] (0.55 mmol) and 200 μL of 3-hexyne (1.75 mmol) were used. An orange solid was isolated (200 mg, 39% yield).

Anal. Found: C, 40.60; H, 6.03. Calcd for $C_{32}H_{56}O_8W_2$: C, 41.04; H, 6.03. ^{1}H NMR ($C_6D_5CD_3$; 400 MHz): isomer **A**, δ 1.17 (s, 36 H, $O_2CC(CH_3)_3$), 1.26 and 1.35 (both t, 6 H each, C≡CCH$_2$CH_3) 2.72 and 3.10 (both q, 4 H each, C≡CCH_2CH$_3$); isomer **B**, δ 1.12 (s, 36 H, $O_2CC(CH_3)_3$), 1.50 (t, 12 H, X part of ABX_3 spin system, C≡CCH$_2$CH_3), 3.07 and 3.28 (both m, 4 H each, A and B part of ABX_3 spin system, C≡CCH_2CH$_3$). ^{13}C

(23) (a) Chisholm, M. H.; Eichhorn, B. W.; Huffman, J. C. *Organometallics* **1989**, *8*, 80−89. (b) Cotton, F. A.; Schwotzer, W.; Shamshoum, E. S. *Organometallics* **1983**, *2*, 1167−71.

NMR ($C_6D_5CD_3$; 100.6 MHz): isomer **A**, δ 14.31 and 15.08 (both s, C≡CCH_2CH_3), 27.01 (s, $O_2CC(CH_3)_3$), 28.81 and 30.39 (both s, C≡CCH_2CH_3) 40.73 (s, $O_2CC(CH_3)_3$), 184.88 and 188.55 (both s, C≡CCH_2CH_3), 197.03 (s, $O_2CC(CH_3)_3$); isomer **B**, δ 14.61 (s, C≡CCH_2CH_3), 26.93 (s, $O_2CC(CH_3)_3$), 29.55 (s, C≡CCH_2CH_3), 40.67 (s, $O_2CC(CH_3)_3$), 187.14 (s, C≡CCH_2CH_3, J_{WC} = 24 and 34 Hz), 196.97 (s, $O_2CC(CH_3)_3$). ^{1}H NMR (CD_2Cl_2; 400 MHz): isomer **A**, δ 1.15 (s, 36 H, $O_2CC(CH_3)_3$), 1.16 and 1.33 (both t, 6 H each, C≡CCH_2CH_3) 2.71 and 3.08 (both q, 4 H each, C≡CCH_2CH_3); isomer **B**, δ 1.13 (s, 36 H, $O_2CC(CH_3)_3$), 1.24 (t, 12 H, X part of ABX_3 spin system, C≡CCH_2CH_3), 2.77 and 3.06 (both m, 4 H each, A and B part of ABX_3 spin system, C≡CCH_2CH_3). MS (EI): *m*/*z* 936.3 (90%) $(M)^+$.

Preparation of [W_2(κ^2-O_2C^tBu)$_4$(μ-MeCCPh)$_2$]. A 300 mg portion of [$W_2(O_2C^tBu)_4$] (0.39 mmol) and 100 μL of MeC≡CPh (0.80 mmol) were used. A red solid was isolated (133 mg, 34% yield).

Anal. Found: C, 44.72; H, 5.13. Calcd for $C_{38}H_{56}O_8W_2$: C, 45.44; H, 5.22. IR (KBr): $\nu_a(CO_2)$ 1510 cm^{-1}, $\nu_s(CO_2)$ 1432 cm^{-1}. ^{1}H NMR (CD_2Cl_2; 400 MHz): isomer **A**, δ 0.74 (s, 36 H, $O_2CC(CH_3)_3$), 3.01 (s, 6 H, C≡CCH_3), 7.10−7.46 (several m, 10H, C_6H_5); isomer **B**, δ 0.69 and 1.16 (both s, 18 H, $O_2CC(CH_3)_3$), 2.95 (s, 6 H, C≡CCH_3), 7.10−7.46 (several m, 10H, C_6H_5). ^{13}C NMR (CD_2Cl_2; 100.6 MHz): isomer **A**, δ 20.14 (s, C≡CCH_3), 25.89 (s, $O_2CC(CH_3)_3$), 40.34 (s, $O_2CC(CH_3)_3$), 128.81, 128.09, 133.06 and 140.84 (each s, aromatic C_6H_5), 175.70 and 185.13 (both s, Ph*C*≡*C*CH_3), 197.16 (s, $O_2CC(CH_3)_3$); isomer **B**, δ 18.93 (s, C≡CCH_3), 25.77 and 26.41 (both s, $O_2CC(CH_3)_3$), 40.34 and 40.57 (both s, $O_2CC(CH_3)_3$), 128.72, 128.16, 132.40, 141.99 (each s, C_6H_5), 176.23 and 185.02 (both s, Ph*C*≡*C*CH_3), 197.78 and 197.96 (both s, $O_2CC(CH_3)_3$). MS (EI): *m*/*z* 1004.3 (100%) $(M)^+$.

Preparation of [W_2(κ^2-O_2C^tBu)$_4$(μ-PhCCPh)$_2$]. A 116 mg portion of [$W_2(O_2C^tBu)_4$] (0.15 mmol) and 60 mg of PhC≡CPh (0.33 mmol) were used. A total of 60 mg of a purple solid was isolated (35% yield).

Anal. Found: C, 49.30; H, 5.43. Calcd for $C_{38}H_{52}O_8W_2$: C, 51.08; H, 5.00. IR (KBr): $\nu_a(CO_2)$ 1511 cm^{-1}, $\nu_s(CO_2)$ 1431 cm^{-1}. ^{1}H NMR (C_6D_6; 400 MHz): isomer **A**, δ 0.86 (s, 36 H, $O_2CC(CH_3)_3$), 6.83, 7.39 (both t, 8 H, J_{HH} = 7.6 Hz, *m*-C_6H_5), 7.62 and 8.08 (both dd, J_{HH} = 8.0 and 1.5 Hz, *o*-C_6H_5) (not all signals could be clearly identified due to accidental overlap with isomer **B** and free PhC≡CPh); isomer **B**, δ 0.81 (s, 36 H, $O_2CC(CH_3)_3$), 6.94 (t, 4 H, J_{HH} = 7.6 Hz, *p*-C_6H_5), 7.21 (t, 8 H, J_{HH} = 7.6 Hz, *m*-C_6H_5), 8.07 (dd, 4 H, J_{HH} = 1.0 and 7.2 Hz, *o*-C_6H_5). ^{13}C NMR (C_6D_6; 100.6 MHz): isomer **A**, δ 25.81 (s, $O_2CC(CH_3)_3$), 40.38 (s, $O_2CC(CH_3)_3$), 125.61, 127.98, 128.00, 128.32, 128.54, 129.35, 130.15, 133.34 and 145.54 (all s, aromatic C_6H_5), 173.87 and 181.29 (s, C≡*C*C_6H_5), 198.59 (s, $O_2CC(CH_3)_3$); isomer **B**, δ 25.89 (s, $O_2CC(CH_3)_3$), 40.33 (s, $O_2CC(CH_3)_3$), 128.196, 132.15 and 143.27 (180.49 (s, C≡*C*C_6H_5), 198.14 (s, $O_2CC(CH_3)_3$). ^{1}H NMR (CD_2Cl_2; 400 MHz): isomer **B**, δ 0.71 (s, 36 H, $O_2CC(CH_3)_3$), 7.26 (t, 4 H, J_{HH} = 7.6 Hz, *p*-C_6H_5), 7.43 (t, 8 H, J_{HH} = 7.6 Hz, *m*-C_6H_5), 7.67 (dd, 4 H, J_{HH} = 8.2 and 1.2 Hz, *o*-C_6H_5). ^{13}C NMR (CD_2Cl_2; 100.6 MHz): isomer **B**, δ 25.72 (s, $O_2CC(CH_3)_3$), 40.45 (s, $O_2CC(CH_3)_3$), 128.18, 128.99, 132.06 and 142.51 (all s, aromatic C_6H_5) 180.18 (s, C≡*C*C_6H_5, J_{WC} = 19 and 38 Hz), 198.68 (s, $O_2CC(CH_3)_3$). MS (EI): *m*/*z* 1128.5 (100%) $(M)^+$.

Gaussian 98 DFT Calculations. Molecular and electronic structure determinations were performed under either rigid D_2 or C_{2h} symmetry using the Gaussian 98[20] program, employing the B3LYP[24−26] functional in conjunction with the 6-31G* basis set for H, C, and O[27] and the SDD energy consistent pseudopotential basis set for W.[28] All geometries were fully optimized at the above levels using the default optimization criteria of the program. Orbital analyses were completed with GaussView.[29]

Table 4. Summary of Crystallographic Data for [W_2(κ^2-O_2C^tBu)$_4$(μ-MeCCR)$_2$] (R = Me, Ph)

formula	$C_{28}H_{48}O_8W_2$	$C_{38}H_{52}O_8W_2$
fw	880.36	1004.50
cryst syst	monoclinic	orthorhombic
color	orange	orange
cryst size (mm)	0.15 × 0.19 × 0.23	0.04 × 0.15 × 0.15
space group	$P2_1/n$	*Pbca*
temp (K)	150(2)	150(2)
a (Å)	10.494(1)	11.787(1)
b (Å)	10.264(1)	17.799(2)
c (Å)	15.260(1)	20.226(2)
β (deg)	99.55(1)	
V (Å^3)	1620.83(2)	4243.30(7)
Z	2	4
calcd density (g/cm^3)	1.804	1.572
wavelength (Å)	0.710 73	0.710 73
abs coeff (mm^{-1})	7.134	5.461
θ range (deg)	2.20−27.48	2.29−27.48
no. of rflns collected	36000	45558
no. of indep rflns (R_{int})	3713 (0.0321)	4865 (0.061)
R1(*F*) ($I > 2\sigma(I)$)	0.0159	0.0237
R1(*F*) (all data)	0.0177	0.0422
wR2(F^2) (all data)	0.0367	0.0507
goodness of fit	1.122	1.007

X-ray Crystallography. Crystal data and details of data collection, data processing, structure analysis, and structure refinement are given in Table 4. Single-crystal X-ray diffraction data were collected on a Nonius Kappa CCD diffractometer at 150 K using an Oxford Cryosystems Cryostream Cooler. The data collection strategy was set up to measure a quadrant of reciprocal space for [W_2(κ^2-O_2C^tBu)$_4$(μ-C_2Me_2)$_2$] with a redundancy factor of 4 and an octant of reciprocal space for [W_2(κ^2-O_2C^tBu)$_4$(μ-PhCCMe)$_2$] with a redundancy factor of 4.5, which means that 90% of the reflections were measured at 4 or 4.5 times, respectively. A combination of ψ and ω scans with a frame width of 1.0° was used. Data integration was done with Denzo.[30] Scaling and merging of the data were done with Scalepack.[30] Both structures were solved by the Patterson method with SHELXS-86.[31] Both molecules also sit on a crystallographic inversion center. Full-matrix least-squares refinements based on F^2 were performed in SHELXL-86[31] for [W_2(κ^2-O_2C^tBu)$_4$(μ-C_2Me_2)$_2$] and SHELXL-97[32] for [W_2(κ^2-O_2C^tBu)$_4$(μ-PhCCMe)$_2$]. For the compound [W_2(κ^2-O_2C^tBu)$_4$(μ-PhCCMe)$_2$] there is a region of disordered solvent located about another inversion center. While it looks as if this solvent may be some type of hexane molecule, it was very difficult to model it. Instead, the SQUEEZE[33] option of PLATON[34] was used to deal with this region of density. This program modifies the observed structure factors by subtracting away the contributions to them of the electron density in the disordered regions. This region occupies a total of 440 Å^3 per unit cell, and the electron density removed by this SQUEEZE procedure amounts to 144 electrons/unit cell. The methyl group hydrogen atoms were added at calculated positions using a riding model with U(H) = 1.5[U_{eq}(bonded C atom)]. For each methyl group,

(24) Becke, A. D. *Phys. Rev. A: Gen. Phys.* **1988**, *38*, 3098−3100.
(25) Becke, A. D. *J. Chem. Phys.* **1993**, *98*, 5648−5652.
(26) Lee, C.; Yang, W.; Parr, R. G. *Phys. Rev. B: Condens. Matter* **1988**, *37*, 785−789.
(27) Hehre, W. J.; Radom, L.; Schleyer, P. v. R.; Pople, J. A. *Ab initio Molecular Orbital Theory*; Wiley: New York, 1986.
(28) Andrae, D.; Haeussermann, U.; Dolg, M.; Stoll, H.; Preuss, H. *Theor. Chim. Acta* **1990**, *77*, 123−141.
(29) GaussView 2.1; Gaussian Inc., Pittsburgh, PA, 1998.
(30) Otwinowski, Z.; Minor, W. In *Macromolecular Crystallography*; Carter, J. C. W., Sweet, R. M., Eds.; Academic Press: New York, 1997; Vol. 276, Part A, pp 307−326.
(31) Sheldrick, G. M. *Acta Crystallogr., Sect. A: Found. Crystallogr.* **1990**, *A46*, 467−473.
(32) Sheldrick, G. M. SHELXL-97; Universitat Göttingen, Göttingen, Germany, 1993.
(33) Van der Sluis, P.; Spek, A. L. *Acta Crystallogr., Sect. A: Crystallogr.* **1990**, *A46*, 194−201.
(34) Spek, A. L. PLATON; Utrecht University, Utrecht, The Netherlands, 2001.

the torsion angle which defines its orientation about the C−C bond was refined. The other hydrogen atoms were included in the model at calculated positions using a riding model with $U(\mathrm{H}) = 1.2[U_{eq}(\text{bonded C atom})]$. Neutral atom scattering factors were used and include terms for anomalous dispersion.[35]

Acknowledgment. We thank the Ohio State University for financial support and the Ohio Supercomputing Center for computational resources in carrying out the electronic structure calculations.

(35) *International Tables for Crystallography*; Kluwer Academic Publishers: Dordrecht, The Netherlands, 1992; Vol. C.

Supporting Information Available: Tables of atomic coordinates, thermal parameters, and bond distances and angles for $[W_2(\kappa^2\text{-}O_2C^tBu)_4(\mu\text{-}MeCCMe)_2]$ and $[W_2(\kappa^2\text{-}O_2C^tBu)_4(\mu\text{-}PhCCMe)_2]$. This material is available free of charge via the Internet at http://pubs.acs.org.

OM020074E